1. Panuschai Sribumrung[1], 2. Suksun Nungam[2]

King Mongkut's University of Technology North Bangkok (1)

doi:10.15199/48.2023.12.05

Direct Torque Control of Permanent Magnet Synchronous Motors using Feedback Passivation

Abstract. *Direct torque control of permanent magnet synchronous motor by feedback passivation is proposed in this paper. An error state equation consisting of velocity, torque, and flux is considered. Two schemes of designing feedback passivation are studied. The first scheme is called cascade feedback passivation. This scheme divides the system into subsystems. Each subsystem is iteratively passive by feedback passivation, resulting in a cascade interconnection of these subsystems to ensure the passivity of the overall system. Therefore this scheme is easy to design. However, the subsystems are related, so specifying the control loop dynamics is not easy. The second scheme applies the passivity theorem to the overall system. Although the design is more complicated than the first scheme, the closed-loop dynamics consist of independent subsystems. Therefore it is straightforward to design the loops. Both proposed schemes give rise to second-order linear dynamic of speed loop where the gain constants are determined by the pole-placement technique. The simulation results and the experimental results verify both proposed techniques can guarantee the stability of the system, with fast torque response and low torque ripple due to the use of the switch-vector modulation method.*

Streszczenie. *W artykule zaproponowano bezpośrednie sterowanie momentem obrotowym silnika synchronicznego z magnesami trwałymi poprzez pasywację ze sprzężeniem zwrotnym. Rozważane jest równanie stanu błędu składające się z prędkości, momentu obrotowego i strumienia. Badane są dwa schematy projektowania pasywacji ze sprzężeniem zwrotnym. Pierwszy schemat nazywa się pasywacją kaskadowego sprzężenia zwrotnego. Schemat ten dzieli system na podsystemy. Każdy podsystem jest iteracyjnie pasywny przez pasywację ze sprzężeniem zwrotnym, co skutkuje kaskadowym połączeniem tych podsystemów w celu zapewnienia pasywności całego systemu. Dlatego ten schemat jest łatwy do zaprojektowania. Jednak podsystemy są ze sobą powiązane, więc określenie dynamiki pętli sterowania nie jest łatwe. Drugi schemat stosuje twierdzenie o pasywności do całego systemu. Chociaż projekt jest bardziej skomplikowany niż pierwszy schemat, dynamika w zamkniętej pętli składa się z niezależnych podsystemów. Dlatego projektowanie pętli jest proste. Oba proponowane schematy dają początek liniowej dynamice pętli prędkości drugiego rzędu, w której stałe wzmocnienia są określane techniką umieszczania biegunów. Wyniki symulacji i wyniki eksperymentów potwierdzają, że obie proponowane techniki mogą zagwarantować stabilność systemu, z szybką odpowiedzią momentu obrotowego i niskim tętnieniem momentu obrotowego dzięki zastosowaniu metody modulacji wektora przełączającego.* (***Bezpośrednie sterowanie momentem obrotowym silników synchronicznych z magnesami trwałymi przy użyciu pasywacji ze sprzężeniem zwrotnym***)

Keywords: Feedback Passivation, Permanent Magnet Synchronous Motor (PMSM), Direct Torque Control (DTC)
Słowa kluczowe: Pasywacja sprzężenia zwrotnego, Silnik synchroniczny z magnesami trwałymi (PMSM), Bezpośrednia kontrola momentu obrotowego (DTC)

Introduction

Permanent magnet synchronous motors (PMSMs) are used in many industrial applications due to their high performances, such as high-power density, good torque response, high-power factor, compact, and light-weighted [1]. The advantages mentioned above make researchers more interested in doing research for the best control schemes of the PMSMs. The conventional schemes for high-performance ac motor drives are based on field-oriented control (FOC) [2], which is complicated to control. In 1986, Takahashi proposed a new technique called direct torque control (DTC) [3] for induction machines where torque and flux are controlled directly by selecting a voltage stator vector from a switching table [4,5]. Therefore, the DTC gives a fast torque response with simple implementation. However, the DTC suffers from high torque and flux ripples due to switching frequency variations [6-8]. The most popular method for reducing the torque ripple is space-vector pulse-width modulation-based direct torque control (SVPWM-based DTC) [9,10]. This method makes the switching frequency constant.

Over the past years, more researchers have focused on nonlinear control methods for DTC schemes. The sliding mode control-based DTC is proposed in [11-14]. The advantage of SMC-based DTC is its robustness, but the chattering problem occurs. The Feedback linearization DTC to reduce torque and flux ripples are proposed for IPMSM [15].

In [16-21] predictive DTC has been proposed to increase the control performance and reduce the torque ripple by choosing the proper voltage vector in each control period. Since this method utilizes some kind of switching table as does the conventional DTC, therefore stability analysis is impossible.

Passivity theory is an effective tool for analyzing nonlinear systems. The passive control technique is applied for AC electric machines [22-26]. This technique uses Euler-Lagrange model and Port-Hamiltonian model and the stability analysis is rather complex.

This paper proposes a direct torque control method for permanent magnet synchronous motors using feedback passivation to guarantee the stability of the system. Two schemes of designing feedback passivation are studied. The first scheme is called cascade feedback passivation. This scheme is easy to design. However, specifying the closed-loop dynamics is not simple. The second scheme applies the passivity theorem to the overall system. Although the design is more complicated than the first scheme, the closed loop dynamics consist of independent subsystems, and hence the closed loop performance can be easily specified.

This paper is organized as follows. The model of PMSM is introduced in Section 2. In Section 3 the direct torque control schemes are explained. In section 4 the passivity theorems are presented. Cascade feedback passivation control design and overall system feedback passivation control design are proposed in Sections 5 and 6, respectively. The simulation and experimental results are presented in section 7. Finally, the conclusions are drawn in section 8.

PMSM Model

The model of PMSM in the stationary reference frame is used for this analysis. The voltage and flux linkage equations of the PMSM can be described as

$$\vec{v}_s = R\vec{i}_s + \frac{d\vec{\psi}_s}{dt}, \tag{1}$$

(2) $$\vec{\psi}_s = L\vec{i}_s + \vec{\psi}_r ,$$

where $\vec{v}_s$ and $\vec{i}_s$ are stator voltage and current vector, $\vec{\psi}_s$ and $\vec{\psi}_r$ are stator flux and rotor flux vector, *R* and *L* are stator resistance and stator inductance.

The electromagnetic torque of motor can be expressed in terms of stator flux vector and stator current vector as

(3) $$m_M = \frac{3}{2}\frac{P}{2}\vec{\psi}_s \times \vec{i}_s ,$$

where P is the number of pole and $\times$ denotes the cross product.

From Eq. (3), the derivative of torque equation is as follows:

(4) $$\frac{dm_M}{dt} = \frac{3}{2}\frac{P}{2}\left(\frac{d\vec{\psi}_s}{dt}\times\vec{i}_s + \vec{\psi}_s \times \frac{d\vec{i}_s}{dt}\right).$$

From Eq. (4), the increment of the torque is a function of stator flux vector and stator current vector can be derived from Eq. (1) and Eq. (2) as follows:

(5) $$\frac{d\vec{\psi}_s}{dt} = \vec{v}_s - R\vec{i}_s$$

(6) $$\frac{d\vec{i}_s}{dt} = \frac{1}{L}\left(\vec{v}_s - R\vec{i}_s - \frac{d\vec{\psi}_r}{dt}\right).$$

By substituting Eq. (5) and Eq. (6) into Eq. (4), the derivative of torque equation can be derived as

(7) $$\frac{dm_M}{dt} = \left(K_L\vec{\psi}_r \times \vec{v}_s\right) + \left(-\frac{R}{L}m_M - K_L\vec{\psi}_s \times \frac{d\vec{\psi}_r}{dt}\right),$$

where $K_L = \frac{3}{2}\frac{P}{2}\frac{1}{L}$. The electromagnetic torque can be controlled by the stator voltage vector according to Eq. (7).

The voltage equation and flux linkage equation in the d-q synchronous rotating reference frame can be written as

(8) $$v_d = L\frac{di_d}{dt} + \frac{R}{L}(\psi_{sd} - \psi_r) - \omega_r\psi_{sq} ,$$

(9) $$v_q = L\frac{di_q}{dt} + \frac{R}{L}\psi_{sq} + \omega_r\psi_{sd} ,$$

where v_d and v_q are d-q axis stator voltage, i_d and i_q are d-q axis stator current, ψ_{sd} and ψ_{sq} are flux linkage of d-q axis stator, ψ_r and ω_r are rotor flux linkage and rotor speed, respectively. The relationship between these reference frames is shown in Fig. 1.

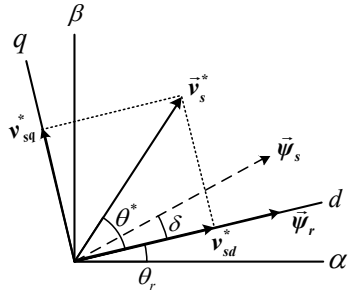

Fig.1. Stator flux and stator voltage component

Direct Torque Control

The concept of direct torque control scheme is to control torque and flux directly. Therefore, this scheme is divided into two parts, namely torque control and stator flux linkage control.

A) Torque Control

In the rotating reference frame, Eq. (7) can be expressed as

(10) $$\frac{dm_M}{dt} = K_L|\vec{\psi}_r|v_q - \frac{R}{L}m_M - K_L|\vec{\psi}_r|\omega_r\psi_{sd} ,$$

where $|\vec{\psi}_r|$ is magnitude of rotor flux linkage.

From Eq. (10), the torque can be controlled by the q-axis stator voltage.

B) Stator flux Control

Eq. (8) can be rearranged as

(11) $$\frac{d\psi_{sd}}{dt} = v_d - \frac{R}{L}(\psi_{sd} - \psi_r) + \omega_r\psi_{sd} .$$

It can be seen from Fig. 1 and Eq. 11 that by controlling ψ_{sd} to be equal to ψ_r, ψ_{sd} can be controlled by v_d. Thus, the state equation of the system is derived from Eq. (10), Eq. (11) and mechanical motion of the motor can be obtained as follows:

(12) $$\frac{d\omega_r}{dt} = \frac{1}{J}(m_M - m_L)$$

where *J* is the inertia and m_L is the load torque.

Passivity Theorems [27]

Consider a dynamic system represented as

(13) $$\dot{x} = f(x,u),$$

(14) $$y = h(x,u),$$

where *f* is locally Lipschitz in (x,u), h is continuous in x, for all $x \in R^n$ and $u \in R^m$ is the control input.

Definition 1 The system of Eq. (13) and Eq. (14) are passive if there exists a continuously differentiable positive definite function $S(x)$ such that

(15) $$u^T y \geq \dot{S}(x) = \frac{\partial S}{\partial x}f(x,u), \forall (x,u) \in R^n \times R^m$$

Moreover, it is said to be output strictly passive if

(16) $$u^T y \geq \dot{S}(x) + y^T\rho(y) \text{ and } y^T\rho(y) > 0, \forall y \neq 0$$

where $S(x)$ is storage function, $u^T y$ is supply rate and $\rho(y)$ is output function.

Definition 2 The system of Eq. (13) and Eq. (14) are said to be zero-state observable if no solution of $\dot{x} = f(x,0)$ can stay identically in $S = \{x \in R^n \mid h(x,0) = 0\}$, other than trivial solution.

Definition 3 The storage function in Eq. (15) is radially unbounded if $\|x\| \to \infty$ then $|S(x)| \to \infty$.

Theorem 1 If the system of Eq. (13) and Eq. (14) are

(1) output strictly passive with a radially unbounded positive definite storage function and

(2) zero-state observable,

then the origin of $x=f(x,0)$ is globally asymptotically stable.

Passivity Cascade Interconnection

Fig. 2 depicts a cascade configuration of interconnected passive subsystems with $n\geq 2$. The overall system will be an input feed-forward passive (IPF) when each subsystem is an output strict passive, as illustrated in Fig 3. Further information can be found in [28].

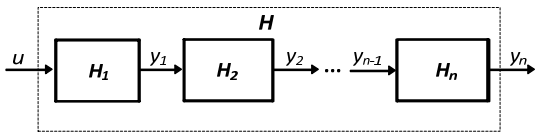

Fig. 2. Cascade Interconnection.

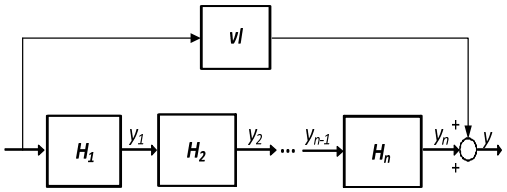

Fig. 3. Feed-Forward Passivation.

Cascade Feedback Passivation Control Design

The cascade feedback passivation control method will be described in this section.

The errors are defined as follows:

$$\begin{aligned} e_\omega &= \omega_r - \omega_r^* \\ e_M &= m_M - m_M^* \\ e_{\psi_d} &= \psi_d - \psi_d^* \end{aligned} \tag{17}$$

where ω_r^*, m_M^* and ψ_d^* are speed, torque and flux commands, respectively.

From Eq. (17), the derivative of error speed equation is as follows:

$$e_\omega = \dot{\omega}_r - \dot{\omega}_r^*. \tag{18}$$

By using Eq. (12) in the error speed equation, the equation can be rewritten as

$$\dot{e}_\omega = \frac{1}{\mathrm{J}}\left(e_m + m_M^* - m_L\right) - \dot{\omega}_r^*. \tag{19}$$

Let us define a positive definite storage function of the error speed equation as

$$S(e_\omega,\vartheta_\omega) = \frac{J}{2}e_\omega^2 + \frac{1}{2}K_{i\omega}\vartheta_\omega^2\ ,\ \vartheta_\omega = \int_0^t e_\omega(\tau)dt. \tag{20}$$

The derivative of Eq. (20) can be expressed as

$$\dot{S}(e_\omega,\vartheta_\omega) = Je_\omega\dot{e}_\omega + K_{i\omega}\vartheta_\omega\dot{\vartheta}_\omega. \tag{21}$$

By substituting Eq. (19) into Eq. (21), the equation can be rewritten as

$$\dot{S}(e_\omega,\vartheta_\omega) = e_\omega\left(\left(e_m + m_M^* - m_L\right) - J\dot{\omega}_r^*\right) + K_{i\omega}\vartheta_\omega\dot{\vartheta}_\omega. \tag{22}$$

Define m_M^* into Eq. (22) in accordance with passive property in theorem 1 as

$$m_M^* = m_L + J\dot{\omega}_r^* - K_\omega e_\omega - \frac{1}{e_\omega}K_{i\omega}\vartheta_\omega\dot{\vartheta}_\omega. \tag{23}$$

By substituting (23) into (22), the equation can be rewritten as

$$\dot{S}(e_\omega,\vartheta_\omega) = e_\omega e_M - K_\omega e_\omega^2. \tag{24}$$

The state equation of subsystem can be represented as

$$H_\omega : \begin{cases} x = f(x,u) \\ y = h(x,u) \end{cases}. \tag{25}$$

Let us define $y = e_\omega$ as the output and $u = e_M$ as the input of speed subsystem, as shown in Fig. 4.

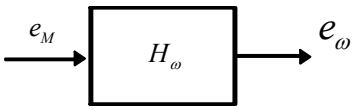

Fig. 4. Speed subsystem

From Eq. (24) it can be shown that;

$$e_\omega e_M \ \geq\ \dot{S}(e_\omega,\vartheta_\omega) + K_\omega e_\omega^2. \tag{26}$$

Thus, the speed subsystem is output strictly passive system corresponding passive property in definition 1, then the zero state observable is investigated.

The stage equation of speed subsystem can be written as

$$\begin{aligned} \dot{\vartheta}_\omega &= e_\omega \\ \dot{e}_\omega &= \frac{1}{J}(e_M - K_\omega e_\omega - K_{i\omega}\vartheta_\omega). \\ \mathrm{y} &= e_\omega \end{aligned} \tag{27}$$

From Eq. (27) and definition 2, with $u = e_M = 0$ and $h(x,u) = h(x,0) = 0$, it can be concluded that

$$y(t)\equiv 0 \Rightarrow e_\omega(t)\equiv 0 \Rightarrow K_{i\omega}\vartheta_\omega(t)\equiv 0 \Rightarrow \vartheta_\omega(t)\equiv 0 \tag{28}$$

Hence, the speed subsystem is zero-state observable. From theorem 1, since storage function is radially unbounded, then this subsystem is globally asymptotically stable. We can also guarantee the stability of the error torque and error d-axe flux stator subsystem in the same manner as above error speed subsystem. The error torque and error d-axis flux subsystem ψ_d^* and v_d are defined, corresponding to passive property in theorem 1 as follows:

$$\begin{aligned} \psi_d^* &= \frac{v_q}{\omega_r} - e_{\psi d} \\ &\quad - \frac{1}{K_L\left|\vec{\psi}_r\right|\omega_r}\left(\frac{R}{L}(e_M + m_M^*) + \dot{m}_M^* - K_M e_M + e_{\psi d}\right) \end{aligned} \tag{29}$$

(30) $$v_d = \frac{R}{L}(e_{\psi d} + \psi_d^* - |\bar{\psi}_r|) - \omega_r \psi_q + \dot{\psi}_d^* - K_\psi e_{\psi d}$$

Therefore, the subsystems can be made passive and globally stable by feedback signals of variables m_M^*, ψ_d^* and v_d. Due to the cascade interconnection of the subsystems, as depicted in Fig 5, the overall system satisfies the passivity of the cascade interconnection property. Therefore, the overall system is globally asymptotically stable.

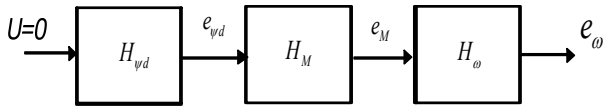

Fig. 5. Cascade passive subsystem of overall system.

From Eq. (29), the control input can be derived as

(31) $$v_q = \frac{R}{L}\frac{e_M}{K_L|\bar{\psi}_r|} + \frac{R}{L}\frac{m_M^*}{K_L|\bar{\psi}_r|} + \omega_r e_{\psi d} + \frac{\dot{m}_M^*}{K_L|\bar{\psi}_r|} - \frac{K_M e_M}{K_L|\bar{\psi}_r|} + \frac{e_{\psi d}}{K_L|\bar{\psi}_r|} + \omega_r \psi_d^* .$$

Thus, the equations (30) and (31) are the final control law of the system.

Cascade Feedback Passivation Closed-Loop Dynamic Design.

The closed-loop dynamic design can be analyzed by the following error state equations:

(32) $$\dot{e}_\omega = -\frac{1}{J}K_\omega e_\omega - \frac{1}{J}K_{i\omega}\vartheta_\omega + \frac{1}{J}e_M$$

(33) $$\dot{\vartheta}_\omega = e_\omega$$

(34) $$\dot{e}_M = e_{\psi d} - K_M e_M$$

(35) $$\dot{e}_{\psi d} = u - K_\psi e_{\psi d} \quad .$$

From Eq. (35), by using u=0, the system can be written in the matrix form as follows:

(36) $$\begin{bmatrix} \dot{e}_\omega \\ \dot{\vartheta}_\omega \\ \dot{e}_M \\ \dot{e}_{\psi d} \end{bmatrix} = \begin{bmatrix} \frac{-K_\omega}{J} & \frac{-K_{i\omega}}{J} & \frac{1}{J} & 0 \\ 1 & 0 & 0 & 0 \\ 0 & 0 & -K_M & 1 \\ 0 & 0 & 0 & -K_\psi \end{bmatrix} \begin{bmatrix} e_\omega \\ \vartheta_\omega \\ e_M \\ e_{\psi d} \end{bmatrix}$$

Since the system matrix, Eq. (36) is linear, from which the torque and flux loops are first order, we propose to select K_ψ and K_M first, then the choice of K_ω and $K_{i\omega}$ can be determined by using pole-placement technique with speed subsystem in Eq. (37).

(37) $$\begin{bmatrix} \dot{e}_\omega \\ \dot{\vartheta}_\omega \end{bmatrix} = \begin{bmatrix} -\frac{1}{J}K_\omega & -\frac{1}{J}K_{i\omega} \\ 1 & 0 \end{bmatrix} \begin{bmatrix} e_\omega \\ \vartheta_\omega \end{bmatrix} + \begin{bmatrix} \frac{1}{J} \\ 0 \end{bmatrix} e_M .$$

The characteristic equation of the speed subsystem is written as

(38) $$\lambda^2 + \frac{1}{J}K_\omega \lambda + \frac{1}{J}K_{i\omega} = 0 \cdot$$

Eq. (38) can be compared with the following standard second-order system:

(39) $$s^2 + 2\zeta\omega_n s + \omega_n^2 = 0 .$$

In this paper, with J = 0.00504 kg-m^2, we choose the settling time to be 0.08 seconds with damping ratio of 0.7. This corresponds to $\omega_n = 71.42$, $K_\omega = 0.5$ and $K_{i\omega} = 25.71$. By choosing $K_M = 1100$ and $K_\Psi = 3000$, the pole of system in the s-plane is shown in Fig. 6.

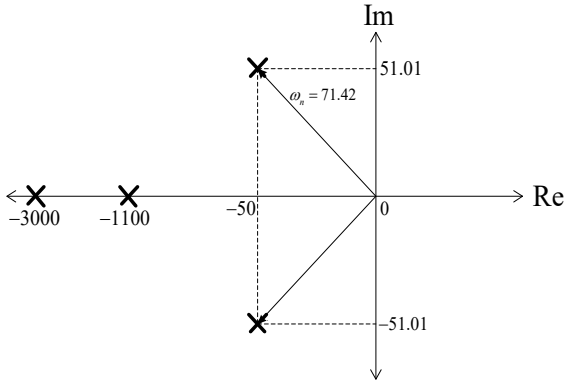

Fig. 6. The pole of system in the s-plane.

The advantage of cascaded feedback passivation control is that the system can be divided into subsystem for analysis which makes it easy to analyse for large system. Nevertheless, specifying the closed loop dynamics is not simple because the subsystems are related. The next section will describe the feedback passivation control design for overall system.

Overall System Feedback Passivation Control Design

The design of overall feedback passivation control begins by defining the following state errors:

(40) $$\dot{e}_{\psi d} = \dot{\psi}_d - \dot{\psi}_d^*$$

(41) $$\dot{\vartheta}_{\psi d} = e_{\psi d}$$

(42) $$\dot{e}_M = \dot{m}_M - \dot{m}_M^*$$

(43) $$\dot{\vartheta}_M = e_M$$

(44) $$\dot{e}_\omega = \dot{\omega}_r - \dot{\omega}_r^*$$

(45) $$\dot{\vartheta}_\omega = e_\omega .$$

Substituting dynamic system into Eq(40), Eq(42) and Eq(44), the error state equation can be derived as

(46) $$\dot{e}_{\psi d} = v_d - \frac{R}{L}e_{\psi d} - \frac{R}{L}\psi_d^* + \frac{R}{L}|\bar{\psi}_r| + \omega_r \psi_q - \dot{\psi}_d^* ,$$

(47) $$\dot{\vartheta}_{\psi d} = e_{\psi d} ,$$

(48) $$\dot{e}_M = K_L|\bar{\psi}_r|v_q - \frac{R}{L}e_M - \frac{R}{L}m_M^* - K_L|\bar{\psi}_r|\omega_r e_{\psi d} - K_L|\bar{\psi}_r|\omega_r \psi_d^* - \dot{m}_M^* ,$$

(49) $$\dot{\vartheta}_M = e_M,$$

(50) $$\dot{e}_\omega = \frac{1}{J}\left(m_M^* - m_L\right) - \dot{\omega}_r^*,$$

(51) $$\dot{\vartheta}_\omega = e_\omega \ .$$

Define a positive definite storage function of overall systems as

(52) $$S(\vec{e}) = \frac{1}{2}K_{i\psi}\vartheta_{\psi d}^2 + \frac{1}{2}e_{\psi d}^2 + \frac{1}{2}K_{iM}\vartheta_M^2 + \frac{1}{2}e_M^2 + \frac{1}{2}K_{i\omega}\vartheta_\omega^2 + \frac{1}{2}e_\omega^2,$$

which, K_{iM} , $K_{i\psi}$ and $K_{i\omega}$ are defined as positive constant control gains.

The time derivative of Eq. (52) can be expressed as

(53) $$\dot{S}(\vec{e}) = K_{i\psi}\vartheta_{\psi d}\dot{\vartheta}_{\psi d} + e_\psi \dot{e}_\psi + K_{iM}\vartheta_M\dot{\vartheta}_M + e_M\dot{e}_M + K_{i\omega}\vartheta_\omega\dot{\vartheta}_\omega + e_\omega\dot{e}_\omega,$$

where $\vec{e}$ is error vector can be defined as

(54) $$\vec{e} = \begin{bmatrix} e_{\psi d} & \vartheta_{\psi d} & e_M & \vartheta_M & e_\omega & \vartheta_\omega \end{bmatrix}^T.$$

Substituting Eq. (46)-(51) into Eq. (53), the time derivative of storage function can be derived as

(55) $$\begin{aligned}\dot{S}(\vec{e}) = {} & K_{i\psi}\vartheta_{\psi d}\dot{\vartheta}_{\psi d} + K_{i\omega}\vartheta_\omega\dot{\vartheta}_\omega + K_{iM}\vartheta_M\dot{\vartheta}_M \\ & + e_{\psi d}\left(v_d - \frac{R}{L}(e_{\psi d} + \psi_d^* - |\bar{\psi}_r|) + \omega_r\psi_q - \dot{\psi}_d^*\right) \\ & + e_M\left(K_L|\bar{\psi}_r|v_q - \frac{R}{L}(e_M + \dot{m}_M^*)\right) \\ & + e_M\left(-K_L|\bar{\psi}_r|\omega_r(e_{\psi d} + \psi_d^*) - m_M^*\right) \\ & + e_\omega\left(\frac{1}{J}\left(m_M^* - m_L\right) - \omega_r^*\right)\end{aligned}.$$

The overall structure of the system shown in Fig. 7 consists of 3 inputs and 3 outputs. The overall system is passive when the overall system storage function is less than or equal to total supply rate of system. It can be expressed as

(56) $$\dot{S}(\boldsymbol{x}) \le u_1y_1 + u_2y_2 + u_3y_3.$$

The state equation of overall system can be presented as

(57) $$\mathrm{H}_{all}: \begin{cases}\dot{\boldsymbol{x}} = \boldsymbol{f}(\boldsymbol{x},\boldsymbol{u}) \\ \boldsymbol{y} = \boldsymbol{h}(\boldsymbol{x},\boldsymbol{u})\end{cases}.$$

By defining the input system as $u_1 = e_{\psi d}^*$, $u_2 = e_M^*$, $u_3 = e_\omega^*$ and the output system as $y_1 = e_{\psi d}$, $y_2 = e_M$, $y_3 = e_\omega$, the Eq. (56) is obtained as follows:

(58) $$\dot{S}(\boldsymbol{x}) \le e_{\psi d}^* e_{\psi d} + e_M^* e_M + e_\omega^* e_\omega.$$

The system will be passive if we choose v_d , v_q and m_M^* in Eq. (55) as follows:

(59) $$\begin{aligned} v_d = {} & \frac{R}{L}(e_{\psi d} + \psi_{sd}^* - |\bar{\psi}_r|) - \omega_r\psi_{sq} \\ & - K_{i\psi}\vartheta_{\psi d} - K_\psi e_{\psi d} + \dot{\psi}_{sd}^* + e_{\psi d}^* \end{aligned}$$

(60) $$\begin{aligned} v_q = {} & \frac{1}{K_L|\bar{\psi}_r|}\left(\frac{R}{L}e_M + K_L|\bar{\psi}_r|\omega_r e_{\psi d}\right. \\ & + K_L|\bar{\psi}_r|\omega_r\psi_{sd}^* - K_{iM}\vartheta_M \\ & \left. - K_M e_M + \dot{m}_M^* + e_M^* + \frac{R}{L}m_M^*\right) \end{aligned}$$

(61) $$m_M^* = J\left(\dot{\omega}_r^* + \frac{1}{J}m_L - K_{i\omega}\vartheta_\omega - K_\omega e_\omega + e_\omega^*\right).$$

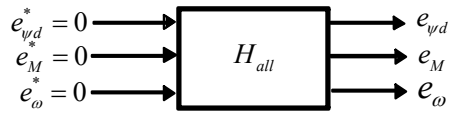

Fig. 7. Control structure of the overall system.

By substituting Eq. (59), Eq. (60) and Eq. (61) into Eq. (55), the equation can be rewritten as

(62) $$\dot{S}(\vec{e}) + K_\psi e_{\psi d}^2 + K_M e_M^2 + K_\omega e_\omega^2 = e_{\psi d}^* e_{\psi d} + e_M^* e_M + e_\omega^* e_\omega.$$

The Eq. (62) corresponds with Eq. (58). Thus, the whole system is output strictly passive system. Then zero-state observable needs to be verified to guarantee the stability in accordance with theorem 1.

The error of the overall system can be represented in the following form,

(63) $$H_{all}: \begin{cases}\dot{x} = f(x,u) \\ y = h(x,u)\end{cases}.$$

Substituting v_d , v_q and m_M^* into Eq.(46), Eq.(48) and Eq.(50) results in the error state equation and output of the system as

(64)
$$\begin{bmatrix}\dot{e}_\omega \\ \dot{\vartheta}_\omega \\ \dot{e}_M \\ \dot{\vartheta}_M \\ \dot{e}_{\psi d} \\ \dot{\vartheta}_{\psi d}\end{bmatrix} = \begin{bmatrix}-K_\omega & -K_{i\omega} & 0 & 0 & 0 & 0 \\ 1 & 0 & 0 & 0 & 0 & 0 \\ 0 & 0 & -K_M & -K_{iM} & 0 & 0 \\ 0 & 0 & 1 & 0 & 0 & 0 \\ 0 & 0 & 0 & 0 & -K_\psi & -K_{i\psi} \\ 0 & 0 & 0 & 0 & 1 & 0\end{bmatrix}\begin{bmatrix}e_\omega \\ \vartheta_\omega \\ e_M \\ \vartheta_M \\ e_{\psi d} \\ \vartheta_{\psi d}\end{bmatrix} + \begin{bmatrix}1 & 0 & 0 & 0 & 0 & 0 \\ 0 & 0 & 0 & 0 & 0 & 0 \\ 0 & 0 & 1 & 0 & 0 & 0 \\ 0 & 0 & 0 & 0 & 0 & 0 \\ 0 & 0 & 0 & 0 & 1 & 0 \\ 0 & 0 & 0 & 0 & 0 & 0\end{bmatrix}\begin{bmatrix}e_\omega^* \\ \vartheta_\omega \\ e_M^* \\ \vartheta_M \\ e_{\psi d}^* \\ \vartheta_{\psi d}\end{bmatrix},$$

$$y = \begin{bmatrix}y_1 \\ y_2 \\ y_3\end{bmatrix} = \begin{bmatrix}1 & 0 & 0 & 0 & 0 & 0 \\ 0 & 0 & 1 & 0 & 0 & 0 \\ 0 & 0 & 0 & 0 & 1 & 0\end{bmatrix}\begin{bmatrix}e_\omega \\ \vartheta_\omega \\ e_M \\ \vartheta_M \\ e_{\psi d} \\ \vartheta_{\psi d}\end{bmatrix} + \begin{bmatrix}e_\omega^* \\ e_M^* \\ e_{\psi d}^*\end{bmatrix}.$$

From Eq. (64), it can be clearly seen that the subsystems are independent. Therefore the zero state observable can be verified for each subsystem.

Substituting v_d into Eq. (46), the error state equation and output of subsystem $\dot{e}_{\psi d}$ are obtained as follows:

(65) $$\dot{\vartheta}_{\psi d} = e_{\psi d}$$

(66) $$\dot{e}_{\psi d} = -K_{i\psi}\vartheta_{\psi d} - K_\psi e_{\psi d} + e_{\psi d}^*$$

(67) $y_1 = e_{\psi d}$

From definition 2, when $u = e^*_{\psi d} = 0$ and $h(x,u) = h(x,0) = 0$, therefore,

$$y_1(t) \equiv 0 \Rightarrow e_{\psi d}(t) \equiv 0 \Rightarrow K_{i\psi} \vartheta_{\psi d}(t) \equiv 0 \Rightarrow \vartheta_{\psi d}(t) \equiv 0.$$

Hence, the subsystem $\dot{e}_{\psi d}$ is zero-state observable. Thus, the subsystem is globally asymptotically stable.

We can verify the zero-state observable of the error torque and error d-axe flux stator subsystem in the same manner as above error speed subsystem. Therefore, overall system is zero-state observable with a storage function is radially unbounded, then over all system will be globally asymptotically stable corresponding theorem 1.

Therefore, m^*_M, v_d and v_q are the feedback signals that make the subsystems passive and globally stable.

The closed-loop dynamics design can be analyzed using second-order linear system, where the gain constants are determined by pole-placement technique. It is straightforward to design the closed-loop dynamics because the subsystems are independent.

To obtain the final control law for the proposed scheme, one can use Eq. (30) and Eq. (31) for cascade feedback passivation control, and Eq. (59) and Eq. (60) for overall feedback passivation control. The control structure diagram is shown in Fig. 8.

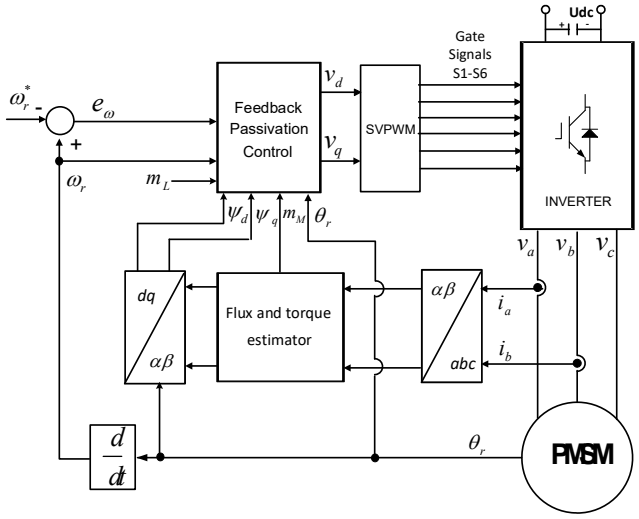

Fig. 8. Feedback passivation control structure.

Simulation and Experimental Results

A) Simulation Results

In this section, the evaluation of the control performance of the proposed scheme has been conducted through simulation using Matlab-Simulink software. The parameters of the PMSM are listed in Table1.

Table 1. Parameters of PMSM

Symbol	Description	Value
P_N	Rated power	2.26 kW
V	Rated voltage	240 V
A	Rated current	4.4 A
R	Stator resistance	0.9 Ω
L	Stator inductance	5.325 mH
P	Number of pole	6
ψ_r	Permanent magnet flux	0.3347 Wb
J	Moment of inertia	0.00504 kg.m^2

The simulation results of two proposed methods are shown as follows.

1) Cascade feedback passivation control

The control parameters adopted in the simulation are reported in Table 2.

Table 2. Control parameters of cascade feedback passivation

Control parameter	gain
K_ω	0.5
$K_{i\omega}$	0.027
K_M	1100
K_Y	3000

The control parameters K_ω and $K_{i\omega}$ are the gain of speed control loop, K_M and K_Y are the gain of torque and stator flux loop.

Fig. 9 and Fig. 10 show the speed responses when the reference speed changing from 100 to 200 rpm and 100 to 300 rpm respectively. Notice that the control parameter K_ω and $K_{i\omega}$ are low values, which makes no overshoot for the transient response. The simulation result of the torque response of reference speeds 200 rpm at 0.4s load are applied as 1.5 Nm and 2 Nm are shown in Fig. 11 and Fig. 12.

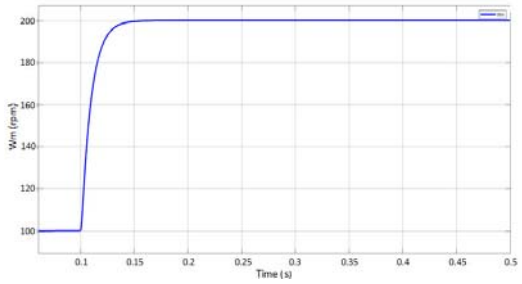

Fig. 9. Simulation speed response reference from 100 to 200 rpm.

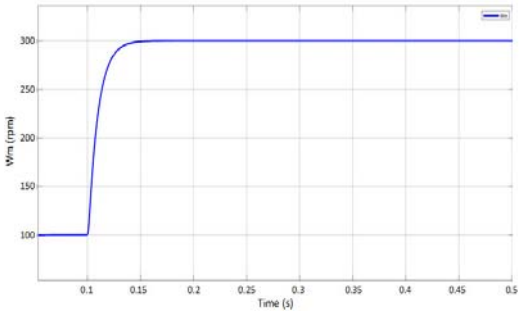

Fig. 10. Simulation speed response reference from 100 to 300 rpm.

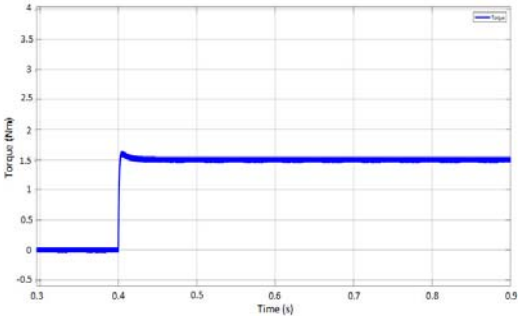

Fig. 11. Simulation torque response 1.5 Nm at 200 rpm.

The speed response for cascade feedback passivation control is shown in Fig. 13 with settling time 0.08s. The control parameter derived from the pole-placement technique are listed in Table 3.

Table 3. Control parameters of cascade feedback passivation settling time 0.08s

Control parameter	gain
K_{ω}	0.5
$K_{i\omega}$	25.71
K_{M}	1100
K_{Y}	3000

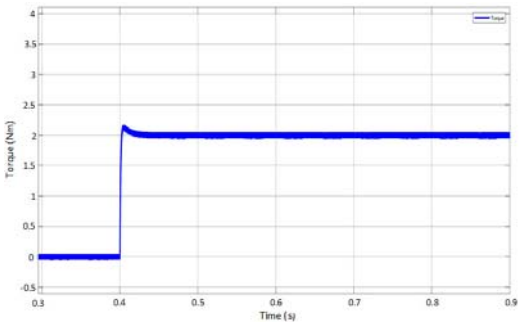

Fig. 12. Simulation torque response 2 Nm at 200 rpm.

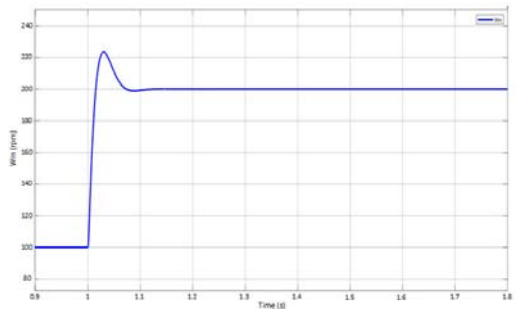

Fig. 13. Settling time 0.08s at 200 rpm of cascade feedback passivation control.

2) Overall feedback passivation control

For the simulation of overall feedback passivation control, the parameters are acquired in the same manner. The parameters for the speed response with settling time of 0.08s, 0.13s and 0.4s are listed in Table 4.

Table 4. Control parameters of overall feedback passivation

Control parameter	Gain(0.08s.)	Gain(0.13s.)	Gain(0.4s.)
K_{ω}	100	61.53	20
$K_{i\omega}$	5101.95	1932.12	204.06
K_{M}	1100	1100	1100
K_{iM}	0	0	0
K_{ψ}	3000	3000	3000
$K_{i\psi}$	0	0	0

The result of settling time speed response 0.08s, 0.13s and 0.4s are presented in Fig. 14, Fig. 15 and Fig. 16, respectively.

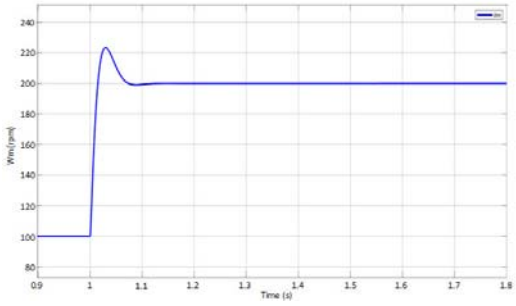

Fig. 14. Settling time response 0.08s of overall feedback passivation control.

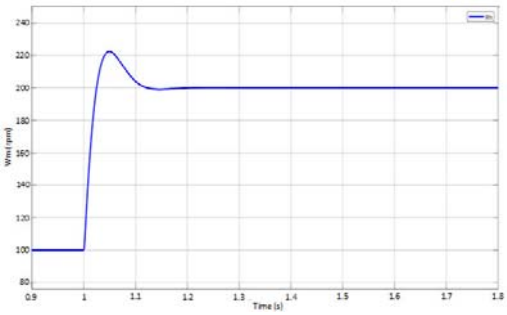

Fig. 15. Settling time response 0.13s of overall feedback passivation control.

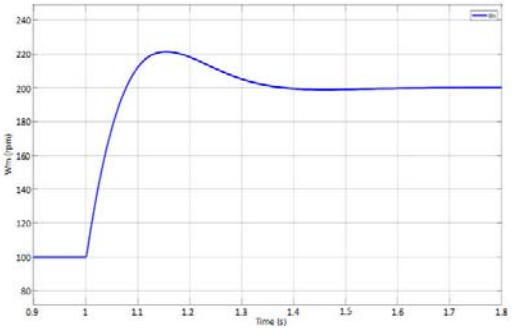

Fig. 16. Settling time response 0.4s of overall feedback passivation control.

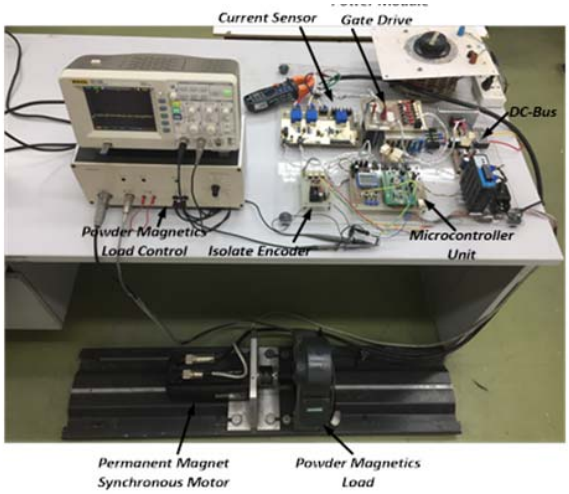

Fig. 17. Experimental setup.

B) Experimental Results

Both of the proposed schemes are implemented using the STM32F4-Discovery board. The switching devices are voltage source inverter that employs the package IGBT module. The switching frequency is 10kHz. The

experimental setup is illustrated in Fig. 17. The experimental parameters are the same as those used in the simulation to verify the proposed schemes.

1) Cascade feedback passivation control

The experimental result when speed changes from 100 to 200 rpm is shown in Fig. 18. Fig. 19 shows the experimental result of speed changes from 100 to 300 rpm. Fig. 20 shows the settling time speed response of 0.08s. The experimental result of torque response due to the incremental load change of 1.5 Nm, and 2 Nm are presented in Fig. 21 and Fig. 22, respectively.

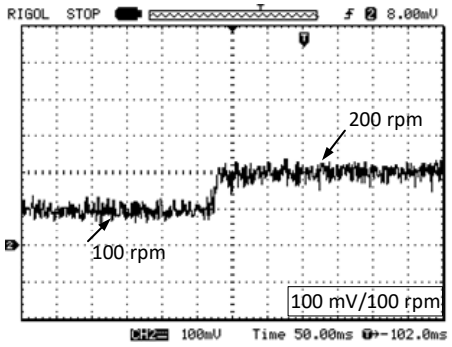

Fig. 18. Experimental result of speed response 100 to 200 rpm.

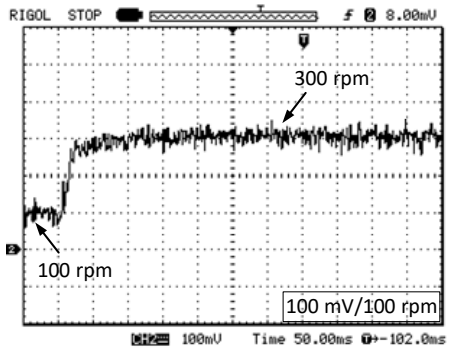

Fig. 19. Experimental result of speed response 100 to 300 rpm.

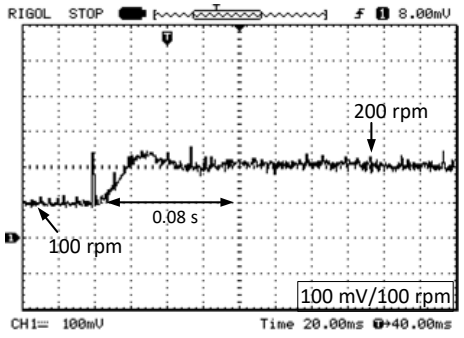

Fig. 20. Experimental result of speed response, settling time 0.08s.

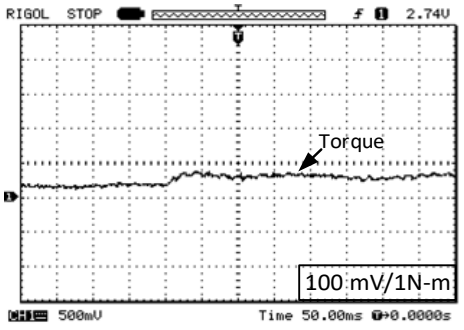

Fig. 21. Experimental result of torque response 1.5 Nm.

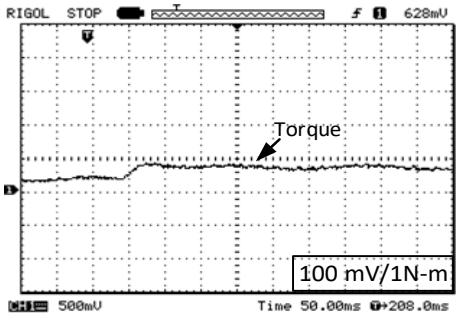

Fig. 22. Experimental result of torque response 2 Nm.

2) Overall feedback passivation control

The experimental result of speed changes from 100 to 200 rpm of overall feedback passivation control, the parameter closed-loop are designed, consisting of K_{ω}, $K_{i\omega}$, K_M, K_{iM}, K_{ψ}, and $K_{i\psi}$. The speed gain control K_{ω}, and $K_{i\omega}$ are designed for settling time of 0.08s, 0.13s, and, 0.4s, and the speed responses are shown in Fig. 23, Fig.24 and Fig.25, respectively.

According to both proposed scheme results, the proposed control design techniques can implement closed-loop dynamics of the system effectively.

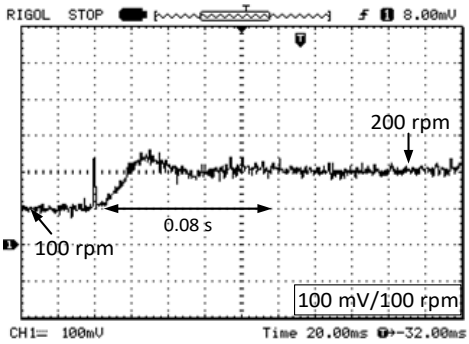

Fig. 23. Experimental result of speed response, settling time 0.08s of overall feedback passivation control.

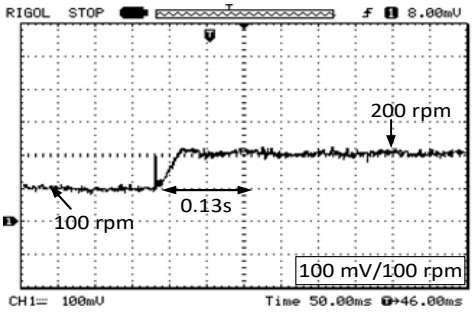

Fig. 24. Experimental result of speed response, settling time 0.13s of overall feedback passivation control.

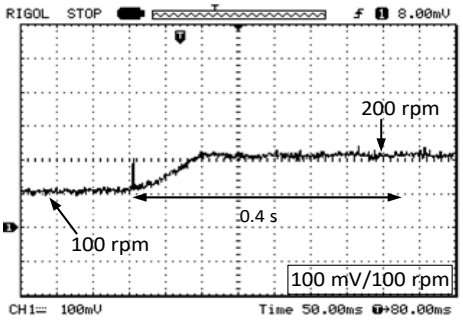

Fig. 25. Experimental result of speed response, settling time 0.4s of overall feedback passivation control.

Conclusions

In this paper, feedback passivation techniques for PMSM based on direct torque control have been presented. The techniques can guarantee the stability of the system effectively. Two scheme are preposed. The first scheme is cascade feedback passivation. This scheme divides the system into a subsystem, where feedback can make each subsystem globally asymptotically stable. The speed, torque, and flux are analyzed as subsystems connected in a cascade. The stability analysis of the overall system becomes easy, but the dynamic closed-loop design is challenging because the subsystems are interrelated. Therefore the second scheme, the overall feedback passivation, is proposed by consider the overall system as passive. Although the analysis is more complicated than the first scheme, the closed-loop dynamics comprises independent subsystems. As a result, it is straightforward to design the loop. The pole-placement technique is utilized to determine the speed loop gain constants of both proposed schemes. The parameter gain constant consisted of K_{ω}, $K_{i\omega}$, K_{M}, K_{iM}, K_{ψ}, and $K_{i\psi}$. The simulation and experimental results show that both proposed techniques can guarantee the stability of the system, with fast torque response and low torque ripple.

***Authors**: Mr.Panuschai Sribumrung, E-mail: panuschai1@gmail.com; Assoc.Prof.Dr. Suksun Nungam, E-mail: suksunnungam@gmail.com, Department of Electrical and Computer Engineering, King Mongkut's University of Technology North Bangkok (KMUTNB), 1518 Wong Sang Bangsue District, Bangkok, Thailand.*

REFERENCES

[1] R. Krishnan, Permanent Magnet Synchronous and Brushless DC Motor: CRC Press. 2010.

[2] F. Blaschke., Johnson B., The principle of field orientation as applied to new TRANSVECTOR close loop control system for rotation field machines: Siemens Review, Vol.39, No.5, 217-220

[3] I. Takahashi and T. Noguchi, A new quick-response and high efficiency control strategy of an induction motor, *IEEE Trans Ind. Appl*., Vol. 22, No.5, (Sep 1986), 820-827

[4] L. Zhong, F. Rahman, W. Y. Hu and K. W. Lim, Analysis of Direct Torque Control in Permanent Magnet Synchronous Motor Drive, *IEEE Transactions on Power Electronic,* Vol.12, No.3, (May 1997), 528-536

[5] M. H. Vafaie, B. M. Dehkordi, P. Moallem and A. Kiyoumarsi, A New Predictive Direct Torque Control Method for Improving Both Steate-State and Transient-State Operations of the PMSM, *IEEE Transactions on Power Electronics*, Vol.31, No.5, (May 2016), 2738-3753

[6] D. Casadei, F. Profumo, G. Serra and A. Tani, FOC and DTC: Two Viable Schemes for induction Motors Torque Control, *IEEE Transactions on Power Electronics,* Vol.17, No. 5, (September 2002), 779-787

[7] F. Niu, B. Wang, A. S. Babel, K. Li and E. G. Strangas, Comparative Evaluation of Direct Torque Control Strategies for Permanent Magnet Synchronous Machines, *IEEE Transactions on Power Electronics*, Vol. 31, No. 2, (Feb 2016), 1408-1424

[8] G. S. Buja and M. P. Kazmierkowski, Direct Torque Control of PWM Inverter-Fed AC Motor-A Survey, *IEEE Transactions on power Electronics,* Vol.51, No.4, (August 2004), 744-757

[9] T. G. Habetler, F. Profumo, M. Pastorelli, and L. M. Tolbert, Direct torque control of induction machines using space vector modulation, *IEEE Trans. Ind. Appl*., Vol. 28, No. 5, (Sep 1992), 1045-1053

[10] C. Xia, J. Zhao, Y. Yan and T. Shi, A novel direct torque control of matrix converter-fed PMSM drives using duty cycle control for torque ripple reduction, *IEEE Trans Ind. Electron*., Vol. 61, No. 6, (Jun 2014), 2700-2713

[11] A. A. Hassan, Y. S. Mohamad and E. G. Shehata, Direct torque control of an ipmsm drive based on sliding mode technique, *Eleventh International Middle East Power System Conference*, Vol. 1, (2006), 10-17

[12] Z. Chen, X. D. Lui and D. P. Yang, Dynamic sliding mode control for direct torque control of PMSM base on expected space vector modulation, *In Proc. 2nd Int. Conf. Syst*, Vol. 1, 2010, 394-397

[13] S. Z. Chen, N. C. Cheung, K. C. Wong and J. Wu, Integral sliding-mode direct torque control of doubly-fed induction generators under unbalanced grid voltage, *IEEE Trans. Energy Convers*., Vol. 25, No. 2, (Jun. 2010), 356-368.

[14] G. H. B. Foo and M. F. Rahman, Direct torque control of an IPM-synchronous motor drive at very low speed using a sliding-mode stator flux observer, *IEEE Trans. Power Electron*., Vol. 25, No. 4, (Apr. 2010), 933-942.

[15] Y.S. Choi, H. H. Choi and J. W Jung, Feedback linearization direct torque control with reduced torque and flux ripples for ipmsm drives, *IEEE Trans. Ind. Appl*, Vol. 31, No. 5, (May 2016), 3728-3737

[16] M. Pacas and J. Weber, Predictive direct torque control for PM synchronous machine, *IEEE Trans. Ind. Electron*., Vol. 52, No. 5, (Oct. 2005), 1350-1356.

[17] T. Gyer, G. Papafotiou and M. Morari, Model predictive direct torque control -partI: Concept, algorithm and analysis, *IEEE Trans. Power Electron*, Vol. 56, No. 6, (Jun. 2009), 1894-1905

[18] H. Zhu, X. Xiao and Y. Li,Torque ripple reduction of the torque predictive control scheme for permanent magnet synchronous motor, *IEEE Trans Ind. Electron.*, Vol. 59, No. 2, (Feb. 2012), 871-877

[19] M. Preindl and S. Bolognani, Model predictive direct torque control with finite control set for PMSM drive systems, part 1: Maximum torque per ampere operation, *IEEE Trans. Ind. Inf*, Vol. 9, No. 4, (Nov. 2013), 1912-1921

[20] Y. Zhang and J. Zhu, A novel duty cycle control strategy to reduce both torque and flux ripple for DTC of permanent magnet synchronous motor drives with switching frequency reduction, *IEEE Trans. Power Electron*, Vol. 26, No. 10, (Oct. 2011), 3055-3067

[21] Y. Cho, K. B. Lee, M. Lin, J. H. Song and Y. I. Lee, Torque-ripple minimization and fast dynamic scheme for torque predictive control of permanent-magnet synchronous motors, *IEEE Trans. Power Electron*., Vol. 30, No. 4, (Apr. 2015), 2182-2190

[22] R. Ortega. G. E. Perez and A. Astolfi. Theory for the user and application examples of the passivity-base control for ac electric machine, *IEEE International Symposium on Industrial Electronics*, (2012), 758-763

[23] H. Xue and Y. Wang. Passivity-based control of synchronous motor. *IEEE PES Innovative Smart Grid Technologies Europe (ISGT Europe)*, Berlin, Germany, (2012), 1-5

[24] R. Mocanu and A. Onea, Passivity Base Torque Control of PMSM used in Electrical Vehicles*, International Conference on System Theory. Control and Computing (ICSTCC)*, Cheile Gradistei Romania, (2015), 803-810

[25] J. Qui and G. Zhao, PMSM Control with Port-Controlled Hamiltonian Theory, *First International Conference on Innovative Computing, Information and Control (ICICIC'06)*, Beijing, China, (2006), 275-278

[26] X. Liu, H. Yu, J. Yu and Y. Zhao., A Novel Speed Control Method Based on Port-Controlled Hamiltonian and Disturbance Observer for PMSM Drives, *IEEE Access*, (2019), Vol. 7, 111115-1111123

[27] Khalil K. H., Nonlinear System, Upper Saddle River, NJ, Prentice-Hall, 2002.

[28] H. Yu and P. J. Antsaklis, A passivity measure of system in cascade based in passivity indices, *IEEE Conference on Decision and Control*, (Dec 2010), 2186-2191